



A model for electric field enhancement in lightning leader tips to levels allowing X-ray and γ ray emissions

Babich, L. P.; Bochkov, E. I.; Kutsyk, I. M.; Neubert, Torsten; Chanrion, Olivier Arnaud

Published in:
Journal of Geophysical Research: Space Physics

Link to article, DOI:
[10.1002/2014JA020923](https://doi.org/10.1002/2014JA020923)

Publication date:
2015

Document Version
Publisher's PDF, also known as Version of record

[Link back to DTU Orbit](#)

Citation (APA):
Babich, L. P., Bochkov, E. I., Kutsyk, I. M., Neubert, T., & Chanrion, O. A. (2015). A model for electric field enhancement in lightning leader tips to levels allowing X-ray and γ ray emissions. *Journal of Geophysical Research: Space Physics*, 120(6), 5087-5100. <https://doi.org/10.1002/2014JA020923>

General rights

Copyright and moral rights for the publications made accessible in the public portal are retained by the authors and/or other copyright owners and it is a condition of accessing publications that users recognise and abide by the legal requirements associated with these rights.

- Users may download and print one copy of any publication from the public portal for the purpose of private study or research.
- You may not further distribute the material or use it for any profit-making activity or commercial gain
- You may freely distribute the URL identifying the publication in the public portal

If you believe that this document breaches copyright please contact us providing details, and we will remove access to the work immediately and investigate your claim.



RESEARCH ARTICLE

10.1002/2014JA020923

Key Point:

• Model of X-ray generation in lightning leader

Correspondence to:

L. P. Babich,
babich@elph.vniief.ru

Citation:

Babich, L. P., E. I. Bochkov, I. M. Kutsyk, T. Neubert, and O. Chanrion (2015), A model for electric field enhancement in lightning leader tips to levels allowing X-ray and γ ray emissions, *J. Geophys. Res. Space Physics*, 120, 5087–5100, doi:10.1002/2014JA020923.

Received 18 DEC 2014

Accepted 12 APR 2015

Accepted article online 15 APR 2015

Published online 12 JUN 2015

A model for electric field enhancement in lightning leader tips to levels allowing X-ray and γ ray emissions

L. P. Babich¹, E. I. Bochkov¹, I. M. Kutsyk¹, T. Neubert², and O. Chanrion²

¹Russian Federal Nuclear Center—VNIIEF, Sarov, Russia, ²Department of Solar System Physics, National Space Institute, Technical University of Denmark, Kongens Lyngby, Denmark

Abstract A model is proposed capable of accounting for the local electric field increase in front of the lightning stepped leader up to magnitudes allowing front electrons to overcome the runaway energy threshold and thus to initiate relativistic runaway electron avalanches capable of generating X-ray and γ ray bursts observed in negative lightning leader. The model is based on an idea that an ionization wave, propagating in a preionized channel, is being focused, such that its front remains narrow and the front electric field is being enhanced. It is proposed that when a space leader segment, formed ahead of a negative lightning leader, connects to the leader, the electric potential of the leader is transferred through the space leader in an ionizing wave that continues into the partly ionized channels of preexisting streamers limit the lateral expansion of the ionization wave, thereby enhancing the peak electric field to values allowing an acceleration of low-energy electrons into the runaway regime where electrons efficiently generate bremsstrahlung. The results suggest that the inhomogeneous ionization environment at the new leader tip amplifies the production rate of energetic electrons relative to a homogeneous environment considered in the past studies.

1. Introduction

The hypothesis by *Wilson* [1924] that postulated acceleration of electrons to high energies in thundercloud electric fields presently is worldwide recognized owing to the well-documented detections of terrestrial gamma ray flashes (TGFs) in the near space [*Fishman et al.*, 1994; *Smith et al.*, 2005; *Briggs et al.*, 2010, 2011; *Tavani et al.*, 2011] and X-ray and γ ray enhancements detected in situ experiments with balloons, aboard airplane, and at the Earth's surface at the sea level and at mountain altitudes [*Shaw*, 1967; *McCarthy and Parks*, 1985; *Suszcynsky et al.*, 1996; *Eack et al.*, 1996a, 1996b, 2000; *Brunetti et al.*, 2000; *Khaerdinov et al.*, 2005; *Chilingarian et al.*, 2009, 2011; *Chilingaryan et al.*, 2010; *Torii et al.*, 2009, 2011; *Tsuchiya et al.*, 2007, 2009, 2011, 2012]. These events, with photon spectra extending up to tens MeV, last from hundreds microsecond [*Briggs et al.*, 2010] up to minutes [*Tsuchiya et al.*, 2007]. They mainly precede the lightning activity, although there are evidences that some TGFs occur after the lightning electromagnetic pulses (EMPs) [*Cummer et al.*, 2005; *Cohen et al.*, 2006]. The origin of these high-energy phenomena is understood in the framework of experimentally proven numerical models [e.g., *Lehtinen et al.*, 1999; *Dwyer and Smith*, 2005; *Gurevich et al.*, 2007; *Babich et al.*, 2008, 2010; *Dwyer*, 2012, and citations therein], assuming a development of relativistic runaway electron avalanches (RREAs) [*Gurevich et al.*, 1992] seeded by cosmic rays in vast and rather long-living thundercloud electric fields whose strength is many times lower not only than the runaway threshold but even than the conventional self-breakdown strength at sea level.

Our paper is devoted to less documented high-energy processes in thunderstorm atmosphere, namely, flashes of penetrating photon emissions observed in direct correlation with EMPs of triggered lightning and in natural negative lightning [*Moore et al.*, 2001; *Dwyer*, 2003a; *Dwyer et al.*, 2004, 2005; *Howard et al.*, 2008]. These flashes are many times narrower than cited above events and last for about $\sim 1 \mu\text{s}$. The photon energies in them are usually around 100 keV, only sometimes up to 1 MeV. The photons, obviously, are bremsstrahlung from microsecond pulses of energetic electrons produced in rather short-living and localized electric field. The observations are puzzling because energetic electrons are generally thought not to be present in conventional gas discharges. Electric discharges in the atmosphere are powered by

©2015. The Authors.

This is an open access article under the terms of the Creative Commons Attribution-NonCommercial-NoDerivs License, which permits use and distribution in any medium, provided the original work is properly cited, the use is non-commercial and no modifications or adaptations are made.

electric fields that accelerate free electrons to energies around 15 eV, where secondary electrons are created through impact ionization of N_2 and O_2 or indirectly by photoionization of O_2 by photons emitted by excited N_2 . The production and loss of free electrons depend on a magnitude of the electric field strength. The threshold electric field, E_k , for a discharge is where sources (ionization) equal losses (attachment of free electrons to O_2 molecules, recombination, etc.). At sea level pressures, the E_k is typically of 32 kV/cm. The bulk of free electrons in a discharge are usually at energies below a few eV, with the tail of the energy distribution function reaching above the ionization threshold and sustaining the discharge. Clearly, these energies are not sufficient to generate X-rays.

The electron energy losses generally increase with electron energy reaching in the atmosphere, a maximum at the electron $\varepsilon \sim 150$ eV [Peterson and Green, 1968]. At higher energies the losses decrease until about 1 MeV where they start to increase energy again. It means that the frictional force, $F(\varepsilon)$, exerted by the atmosphere through the electron collisions with air molecules, varies in the same manner. To accelerate the low-energy electrons to high energies, the electric field strength must be of 270 kV/cm [Babich and Stankevich, 1972], or $\sim 8E_k$, to overcome the maximum of the frictional force. If such fields exist in discharges, electrons may achieve very high energies because they are accelerated past the maximum and into the so-called runaway regime, where the frictional force decreases with increasing electron energy. Such high fields are difficult to achieve, however, because the ionization creates an electrically good conductor that tends to limit the field. It has been interesting therefore to understand how lightning appears able to generate X-rays and γ rays because it opens to a new aspect of lightning discharges or more generally to the gas discharge.

The phenomenon of high-field runaway in dense gases was first observed in the pioneering series of laboratory experiments about 50 years ago in atmospheric air [Stankevich and Kalinin, 1967; Tarasova and Khudyakova, 1969; Tarasova et al., 1975] and helium at 1 atmosphere pressure [Noggle et al., 1968] using high-voltage pulses with subnanosecond risetimes, which allow overcoming the field limitation imposed by the increasing conductivity. Since then, numerous laboratory experiments have been conducted [e.g., Babich et al., 1990; Babich, 2003, 2005; Babich and Loiko, 2009; Babich et al., 2014a, 2014b].

The first analytical estimate of the fluency of this process in weakly ionized gases was published more than half a century ago by Gurevich [1961] and was followed by more accurate studies, for instance by Babich and Stankevich [1972] which for the first time included space charge effects, Bakhov et al. [2000] and Chanrion and Neubert [2010] adopting a full Monte Carlo and particle-in-cell approach, respectively. However, the mechanism capable of accounting for the impulsive electric field enhancement at the tip of a lightning leader to a level sufficient for generation of intensive fluxes of runaway electrons (REs) is not fully understood.

One process that circumvents the need for high electric fields was proposed by Gurevich et al. [1992]. They considered seed electrons, created with energies in the runaway range by cosmic rays and further accelerated and multiplied in lightning—and thunderstorm electric fields, thereby forming a RREA. While this process may possibly power avalanches and associated emissions in clouds, more recent observations suggest that the mechanism primarily is “thermal runaway” [Gurevich et al., 2007] or, more precisely, “high-field runaway” [Dwyer, 2008], with the source region close to the lightning leader tip [Dwyer et al., 2011]. As noted above, this process is not straightforward because of the high electric fields needed.

A model of electron acceleration at lightning leader tips has been proposed by Moss et al. [2006] and further elaborated by Celestin and Pasko [2011]. It involves the two basic modes of gas discharges: the streamer and the leader. A streamer is an ionization wave that in the atmosphere propagates at velocities approaching magnitudes on the order of 10^9 cm/s (cf., simulations by Celestin and Pasko [2011] with $E = 50$ kV/cm and 1 atm) and where the space charge in the wavefront can lead to magnitudes of electric field strength of several E_k . In the wake, it creates a small-scale filament (of 1 mm or less in radius in the atmosphere at sea level pressure) of enhanced ionization and electric conductivity. Many streamers are thought to be injected from a lightning leader tip and to assist its propagation. A lightning leader propagates slower, has a high degree of ionization, a high electric conductivity, and can carry hundreds of amperes of current. It is created by thermal ionization of the neutral gas in the leader channel. When negative lightning propagates (in a direction opposite to the vector of the electric field strength), it often occurs in steps. In between the steps, a negative leader segment, a so-called space leader, may be formed meters ahead [e.g., Gorin et al., 1976; Reess et al., 1995]. The stepped propagation occurs when the main leader channel connects to the space leader [e.g., Biagi et al., 2010].

In Moss *et al.* [2006] and Celestin and Pasko [2011], a two-step process is proposed. The first step occurs in the streamer fields. The authors believed that “while during the most of expansion dynamics of the streamer the maximum field in the streamer head stays close to $\sim 5 E_k$, just prior to the branching of the streamer, this peak field in the streamer head can reach very high values...” sufficient to accelerate thermal electrons to the runaway energy range. In the second step, the electrons are further accelerated to 10–100 keV and higher when the lightning channel connects to the space stem and transfers its potential to the stem. It then creates an impulsive high electric field at the tip of the stem, which is now the new tip of the lightning channel. The number of REs generated in a streamer corona flash was estimated to $\sim 10^{12}$ – 10^{15} [Moss *et al.*, 2006] and 10^{17} [Celestin and Pasko, 2011], the latter number being in the range thought to be required to explain the γ ray bursts observed from satellites, the terrestrial gamma ray flashes (TGFs) [Dwyer, 2008]. For comparison, Gurevich *et al.* [2007] estimated a production of $\sim 3 \times 10^{12}$ REs in one leader step.

Because the leader-streamer interaction is a very complex process that cannot yet be simulated realistically, estimates are made that are sensitive to assumptions on parameters. Celestin and Pasko [2011], for instance, assumed that the RREA length l_{av} is ~ 7 cm and the avalanche region is $L \sim 1$ m giving $L/l_{av} \sim 15$ avalanche lengths, whereas Gurevich *et al.* [2007] assume $l_{av} \sim 1$ cm and $L \sim 10$ cm (for the head length), which give a total of $L/l_{av} \sim 10$ avalanche lengths with a the field intensity > 200 kV/cm ($\sim 6 E_k$). However, according to Monte Carlo simulations [Babich and Bochkov, 2011; Kutsyk *et al.*, 2012a, 2012b], the avalanche length is ~ 16 cm for 218 kV/cm, which decreases the number of avalanche lengths of the assumed region and thereby the number of REs.

On the other hand, the RREA can continue developing in the weaker electric fields at larger distances away from a leader tip. Therefore, it is more reasonable to avoid addressing the number of RREA lengths and directly estimate the RREA enhancement as $\sim \exp(U_L / \langle \varepsilon_{re} \rangle)$ [Dwyer, 2004]. Here U_L is the available potential drop in the cloud, and $\langle \varepsilon_{re} \rangle$ is the characteristic energy of electrons in the RREA. With $U_L \approx 20$ MV, which Gurevich *et al.* [2007] used in the region where RREA is being developed, and $\langle \varepsilon_{re} \rangle \approx 7$ MeV (valid in the range of small overvoltages $\delta = eE / (F_{min} P)$ below the self-breakdown limit in dry air, inherent for the weak thundercloud fields [Babich *et al.*, 2004; Dwyer, 2003b, 2004, 2007; Kutsyk *et al.*, 2012a, 2012b]), the above formula gives the RREA enhancement of 17. Note, here we do not use the conventional definition of the overvoltage relative to the self-breakdown magnitude $E_k/P \approx 32$ kV/(cm · atm) valid for the homogeneous field in dry air; the overvoltage is defined relative to the minimum $F_{min} \approx 2.18$ keV/(cm · atm) of the electron drag force $F(\varepsilon)$ achieved in air at electron energy ε of 1 MeV. Such definition is convenient for describing the runaway process [Gurevich *et al.*, 1992; Roussel-Dupre *et al.*, 1994; Dwyer, 2003b].

Any proposed model of the increase of the electric field at the leader tip should be consistent with observations, such as those by Howard *et al.* [2008] taken in the nature and Kochkin *et al.* [2012] in the laboratory. Most likely, the EMP registered by Howard *et al.* [2008] is generated as a result of the current jump during the new step formation. The pulse is bipolar, i.e., consists of two peaks. The first peak is positive, lasting ~ 100 ns, and the second peak is negative and ~ 1 μ s. In Figure 4 of Howard *et al.* [2008], the X-rays appear 0.5 μ s after the positive peak maximum. In our opinion, the positive peak is connected with the growth of the leader current during the new step formation when the potential is being carried along the space leader channel, and the longer negative peak is connected with the fading current in the new leader segment. Maybe it is possible to reconcile the data with the model by Celestin and Pasko [2011] if one assumes that the time lag between the EMP and the X-ray onsets is exactly the formation time of the streamer corona. Note, however, that Howard *et al.* [2008] observed that the X-ray source was located below that of the EMP. According to the model by Celestin and Pasko, the positions of the sources should coincide. On the other hand, Howard *et al.* [2008] mention some uncertainty in the X-ray source position; therefore, one cannot be confident while interpreting their observations in the framework of any mechanism. Kochkin *et al.* [2012], who investigated the generation of X-rays in long spark laboratory discharges, observed that the radiation appears not at the stage of the streamer corona development but during a contact of positive and negative streamers.

A consistent model, capable of describing the high-field runaway in front of the lightning leader, should include a development of powerful RREA producing the high-energy bremsstrahlung detected in

correlation with lightning leaders. It is well known that “tip of long leader possesses a potential of ~ 1 MV in laboratory sparks and of ~ 10 MV or even higher in lightning” [Bazelyan and Raizer, 2000, 2001, page 75]. Hence, the voltage in front of the leaders is sufficient for the electron energizing up to the MeV energies; however, to start the RREA development, sufficiently strong electric field is required to produce seed REs. Our goal is more limited than complete describing the high-field runaway process including the RREA development: we only plan to consider the initial stage of the process by demonstrating that electric field at the leader front locally can achieve magnitudes allowing low-energy electrons to overcome the runaway energy threshold.

2. A New Mechanism of Runaway Electron Generation

According to the deterministic definition, the electric field in the atmosphere at sea level pressures must be $E > E_{\max} \approx 260\text{--}270$ kV/cm $\approx (8.1\text{--}8.4) E_k$ for the low-energy electrons be capable of overcoming the maximum frictional force at ~ 150 eV and efficiently populate the runaway energy range [e.g., Babich and Stankevich, 1972; Babich et al., 1990; Babich, 2003, 2005]. At lower E fields, a deterministic runaway threshold can instead be introduced $\varepsilon_{\text{th,run}}(E)$ as the minimum energy required for electrons to be in the runaway regime at given E . It is usually defined simply from the equation $F(\varepsilon) = eE$ [e.g., Gurevich, 1961; Babich and Stankevich, 1972; Babich et al., 1990; Babich, 1995]. More precise definitions of $\varepsilon_{\text{th,run}}$ are available in Bakhov et al. [2000], Babich and Bochkov [2011], and Kutsyk et al. [2012a, 2012b].

In the stochastic approach, a probability can be calculated for low-energy electrons to be accelerated into the runaway regime [Bakhov et al., 2000; Chanrion and Neubert, 2010]. As E decreases from E_{\max} (where most electrons will be—or are—in the runaway regime), the combined effect of the increase in $\varepsilon_{\text{th,run}}$ (further out in the tail of the thermal electron energy distribution) and increasing difficulty of gaining sufficient energy, the probability for low-energy electrons to be accelerated past $\varepsilon_{\text{th,run}}$ dramatically decreases. For instance, in air at 1 atm, the probability is 10^{-7} and $4 \cdot 10^{-12}$, respectively, for $E = 6 E_k$ (~ 190 kV/cm) and $E = 5 E_k$ (~ 160 kV/cm), in spite of a rather low corresponding energy threshold of $\varepsilon_{\text{th,run}} \sim 277$ eV and 470 eV [Chanrion and Neubert, 2010]. Similarly, studying the runaway process in pure nitrogen at 1 atm [Bakhov et al., 2000], a rate was computed of thermal electrons transition to the runaway mode, i.e., a rate at which thermal electrons are accelerated past so called “stochastic runaway threshold $\varepsilon_{\text{th,run,stoch}}$ ” defined as an energy, above which the probability of an electron to return to the low-energy range is extremely low. Specifically, with $\varepsilon_{\text{th,run,stoch}} = 8$ keV, the computed rate decreases from $8 \cdot 10^{10} \text{ s}^{-1}$ at 400 kV/cm to 10^4 s^{-1} at 240 kV/cm [Bakhov et al., 2000]. At weaker fields, the dependence on E is even stronger. Therefore, for the thermal electron acceleration into the runaway mode to be significant in the framework of the stochastic description of the process, strong fields with intensities of 200 kV/cm ($6.3 E_k$) or higher are required [Bakhov et al., 2000; Chanrion and Neubert, 2010].

The mechanism for a generation of such field magnitudes in the vicinity of the lightning channel tip is at present speculative. According to Bazelyan and Raizer [2000, 2001, page 75], the field at the head of the leader channel does not significantly exceed the self-breakdown limit of ~ 30 kV/cm and is even less inside the channel. It is well known that strong fields are generated in heads of the streamers constituting the streamer corona of the leader; however, it is not clear what the lifetime of such fields is and therefore their efficiency in acceleration, although estimates have been made [Celestin and Pasko, 2011].

Furthermore, assuming a hemispherical approximation of the ionization wavefront D'yakonov and Kocharovsky [1988, 1989] showed that the maximum value of the normal component of the field strength at the streamer front is of the order of a magnitude E_{infr} at which the ionization rate by electron impacts $\nu_{\text{ion}}(E)$, as a function of E , experiences an inflection ($E_{\text{infr}} \sim 5 E_k$ in air), where sharp $\nu_{\text{ion}}(E)$ increase with E changes to extremely weak growth with E . The maximum is first met in the region on the hemispherical space charge sheath that is normal to the background field (the direction of propagation). A further increase in the streamer sheath field leads to an increase of the ionization in the transverse direction relative to the direction of the streamer propagation such that $E_{m,\text{tip}} \sim E_{\text{infr}}$ is met over a larger region of the sheath including the lateral sides. The result is that the velocities of the ionization wave in the longitudinal and transversal directions become almost equal and that the streamer experiences strong transversal expansion, eventually limiting the field intensity at the leader front [Raizer and Simakov, 1998]. This effect has also been demonstrated in numerical simulations [Vitello et al., 1994; Babaeva and Naidis, 1996;

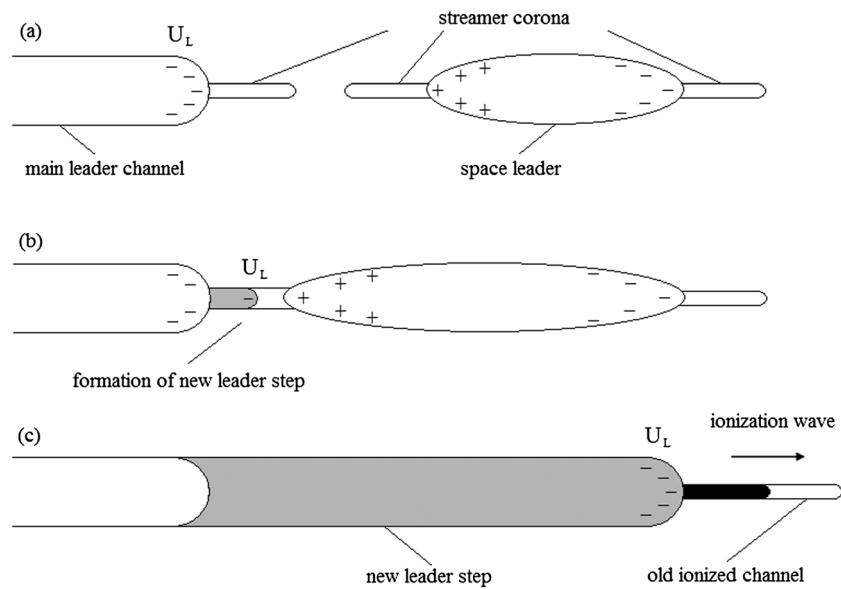


Figure 1. Scenario of negative leader development [Bazelyan and Raizer, 2000]. (a) The main negative leader channel and the space leader channel with their streamer coronas. (b) Contact of the streamer coronas of the main leader (negative) and the space leader (positive) with the potential of the main leader head U_L being transferred to the space leader. (c) The potential of the old main leader is transferred to the negative tip of the space leader, launching an ionization wave propagating into the preexisting streamer channel.

Kulikovsky, 1997, 1998; Celestin and Pasko, 2011]. The overall conclusion from these works is that the steady state magnitude of the field intensity during streamer development in a homogeneous medium does not exceed $150 - 170 \text{ kV/cm} \approx (4.7-5.3)E_k$ at sea level pressures, for which the runaway probability is as low as $4 \cdot 10^{-15} - 10^{-10}$ [Chanrion and Neubert, 2010].

In the model that apparently allows the required fields to develop was proposed by Celestin and Pasko [2011]. They assume that REs are generated during a new leader step formation, where propagation of the electrical potential along the leader channel leads to a formation of streamer corona at a lateral channel surface. During branching of the streamers constituting the corona, the field is being increased up to $\sim 240 \text{ kV/cm}$ at the time of branching.

However, we consider another approach by noting that if the medium is nonuniform from preionized channels formed by previous streamers, the limitation of the electric field magnitude is removed, because a preionized channel tends to focus the ionization wave. A reason of the focusing due to the ionization nonuniformity is as follows. It is known that the lower is the electron density, in which the ionization wave propagates, the lower is the ionization wave velocity. Obviously, the electron density decreases in the direction from the inner areas of the preionized channel to its periphery. Hence, the further is the locus of considered point from the channel axis, the slower develops the ionization process in it. Thereby, the transverse expansion of the ionization wavefront occurs much slower than the longitudinal propagation; therefore, the radius of the front remains to be limited almost to that of the already existing preionized channel, and as a result, the field intensity at the wavefront can reach magnitudes of 240 kV/cm or higher required for the efficient RE generation [Bakhov et al., 2000].

We recall that negative lightning usually propagates in steps with a streamer corona at the tip of the leader as observed in laboratory gas discharges [Bazelyan and Raizer, 2000, 2001, page 77]. At the external boundary of the streamer corona, a plasma is formed, extending in the direction along the electric field vector, from both ends of which streamers start in the directions to and from the leader head (bi-leader). Further, from this plasma, the so-called space leader is formed as described earlier. The space leader with streamer coronas is illustrated in Figure 1a. The positive head of the space leader moves toward the negative head of the main leader channel and at contact, a united conducting channel is being formed where charges are redistributed and the potential of the old leader U_L is transferred to the space leader. The same conceptual framework was described earlier and adopted by Moss et al. [2006] and Celestin and

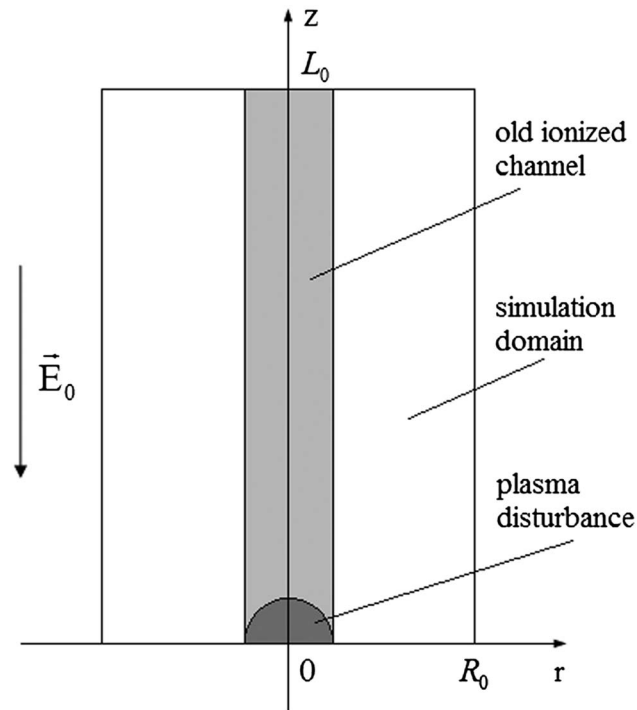


Figure 2. The computational scheme. At $t=0$, the simulation domain ($L_0 = 4$ cm, $R_0 = 6$ mm) is bridged up by the primary ionized channel. Initial spatial distributions of charged particles in the primary channel n_e^{ch} , n_p^{ch} , n_n^{ch} with $n_e^{ch,a,i}$ and $n_p^{ch,a,i}$ at the channel symmetry axis and in plasma disturbance $n_e^{dis} = n_p^{dis}$ with $n_e^{dis,a}$ at the symmetry axis obey equations (2) and (3), respectively, with characteristics longitudinal and transverse sizes $l_z = l_r = 500$ μ m. $E_0 = 50$ kV/cm, $P = 1$ atm.

Pasko [2011]. It is shown in Figure 1b. The potential jump in the body of the space leader will launch new ionization waves propagating along old streamer channels in the negative streamer corona region of the new leader tip, shown in Figure 1c.

We propose therefore that the electric fields can reach amplitudes required to generate bursts of energetic electrons and associated bremsstrahlung in the streamer channels of the space leader. We note that this may happen by the same physical mechanism in the streamers at both ends of the space leader, that is, (1) when opposite polarity streamers, growing toward each other from the main and space leaders, connect and (2) when the potential of the main leader reaches negative pole of the space leader. In the following, we demonstrate the latter case by modeling an ionization wave in a preformed conducting streamer channel.

3. Mathematical Formulation of the Problem

Given the present lack of knowledge of the physical conditions in the leader channels of lightning and of leader-

streamer interactions as mentioned earlier, we limited ourselves to numerical simulations of a generalized channel model relevant for the stage illustrated in Figure 1c, namely, the propagation of a secondary ionization wave along old streamer channels at the time of the potential jump in the body of the space leader. To avoid misunderstanding, it is noted that the earlier stage of collision of the leader and space leader, as in Mallios *et al.* [2013], is not considered. The simulations start at the termination of the motion of the leader step which generates a sharp increase of the external field, E_0 , and a new ionization wave along old streamer channels is initiated.

As according to estimations by Bazelyan and Raizer [2000, 2001, page 76], a radius of the streamer zone (corona) of laboratory long leaders is limited to the magnitudes of ~ 1.5 m at the leader tip potential 1.5 MV, the radius of the streamer zone of the lightning leader, likely, can reach tens of meters. Unfortunately, computers still only allow simulations of streamers a few centimeters in length (at sea level pressures); hence, only the initial stage of the ionization wave propagation can be simulated. According to Bazelyan and Raizer [2000, 2001, page 75], the upper limit of the field at the head of the leader channel does not exceed significantly the self-breakdown limit ~ 30 kV/cm; we assume that voltage jump up to U_L generates at the front of new leader step (Figure 1c) an electric field of 50 kV/cm. This magnitude is taken to be the initial condition on the external field strength throughout the simulation domain.

The problem is formulated in the cylindrical coordinates (z, r) as shown in Figure 2. The simulation domain has the longitudinal and transversal dimensions $L_0 \times R_0$ relative to the vector of static and homogeneous external electric field given by $E_{ext}(\vec{r}) = -E_0 \vec{e}_z$, where \vec{e}_z is a unit vector along the symmetry axis z of the leader. At time $t=0$, this domain is bridged by an ionized channel, where most of the electrons are attached to oxygen molecules. In view of the adopted cylindrical symmetry, the problem is two dimensional.

The kinetics of low-energy electrons (e), positive (p), and negative (n) ions in the discharge is described by the following set of the equations:

$$\begin{aligned} \frac{\partial n_e}{\partial t} + \vec{\nabla} \cdot (n_e \vec{v}_e - D_e \vec{\nabla} n_e) &= (v_{\text{ion}} - v_{\text{att}}) n_e - \beta_{\text{ep}} n_e n_p + S_{\text{ph}}, \\ \frac{\partial n_p}{\partial t} + \text{div} n_p \vec{v}_p &= v_{\text{ion}} n_e - \beta_{\text{ep}} n_e n_p - \beta_{\text{pn}} n_p n_n + S_{\text{ph}}, \\ \frac{\partial n_n}{\partial t} + \text{div} n_n \vec{v}_n &= v_{\text{att}} n_e - \beta_{\text{pn}} n_p n_n, \end{aligned} \quad (1)$$

where n_e , n_p , and n_n are the densities; $\vec{v}_e = -\mu_e \vec{E}$, $\vec{v}_p = \mu_p \vec{E}$, and $\vec{v}_n = -\mu_n \vec{E}$ are the drift velocities, μ_e and $\mu_{p,n}$ are the electron and ion mobilities; D_e is the electron diffusion coefficient; v_{ion} is the ionization rate of the air molecules by impacts of low-energy electrons; β_{ep} and β_{pn} are, respectively, coefficients of recombination of electrons with positive ions and positive and negative ions; $v_{\text{att}} = k_{\text{diss}} N_{\text{O}_2} + k_{\text{thr}} N^2$ is the rate of the electron attachment to the oxygen molecules; k_{diss} and k_{thr} are the rates of dissociative and three-body attachment; N and N_{O_2} are the local densities of air and oxygen molecules at point z ; and S_{ph} is the photoionization source.

The temperatures of the negative ions and the gas as a hole are assumed not to increase during the development time of the simulated process. Therefore, the rate of collisions capable of destroying negative ions is too low for the electron detachment to have significant effect on the electron density (see *Neubert and Chanrion* [2013] for further discussion on electron detachment).

The initial densities of the charged particles in the old streamer channel are set be as follows:

$$\begin{aligned} n_e^{\text{ch}}(z, r) &= n_e^{\text{ch,a,i}} \cdot \exp(-r^2/l_r^2), \\ n_p^{\text{ch}}(z, r) &= n_p^{\text{ch,a,i}} \cdot \exp(-r^2/l_r^2), \\ n_n^{\text{ch}}(z, r) &= n_p^{\text{ch}}(z, r) - n_e^{\text{ch}}(z, r). \end{aligned} \quad (2)$$

Here $n_e^{\text{ch,a,i}}$ and $n_p^{\text{ch,a,i}}$ are the *initial* densities of electrons and positive ions at the streamer *channel* symmetry axis, and l_r is the characteristic width ("radius") of the radial distribution.

To start the ionization wave at the initial moment of time, a cloud of neutral plasma (disturbance) was set in the vicinity of the coordinate onset (Figure 2), consisting of electrons and positive ions with Gaussian spatial distribution of the densities:

$$\begin{aligned} n_e^{\text{dis}}(z, r) &= n_e^{\text{dis,a}} \cdot \exp(-z^2/l_z^2) \cdot \exp(-r^2/l_r^2), \\ n_p^{\text{dis}}(z, r) &= n_e^{\text{dis}}(z, r), \\ n_n^{\text{dis}}(z, r) &= 0, \end{aligned} \quad (3)$$

where the amplitude $n_e^{\text{dis,a}}$ is set equal to 10^{20} m^{-3} throughout the simulations. Merging equations (2) and (3) gives the initial conditions for the set of equation (1):

$$\begin{aligned} n_e(z, r, 0) &= n_e^{\text{ch}}(z, r) + n_e^{\text{dis}}(z, r), \\ n_p(z, r, 0) &= n_p^{\text{ch}}(z, r) + n_p^{\text{dis}}(z, r), \\ n_n(z, r, 0) &= n_n^{\text{ch}}(z, r) + n_n^{\text{dis}}(z, r). \end{aligned} \quad (4)$$

The set in equation (1) was closed by equations for the self-consistent electric field:

$$\begin{aligned} \Delta \phi_{\text{int}} &= -\frac{\rho_q}{\epsilon_0}, \\ \vec{E} &= -\vec{\nabla} \phi_{\text{int}} + \vec{E}_{\text{ext}}, \end{aligned} \quad (5)$$

where ϕ_{int} is the potential of the space charge field produced in the process of the plasma neutrality violation, $\rho_q = e \cdot (n_p - n_n - n_e)$ is the charge density, ϵ_0 is the dielectric permittivity of free space, and e is the elementary charge.

For solving the first equation in (5), the magnitudes of the potential at the border of the computational area are required. The potential in a boundary point \vec{r}_{bound} was computed using the general solution of Poisson equation:

$$\phi_{\text{int}}(\vec{r}_{\text{bound}}) = \frac{1}{4\pi\epsilon_0} \int_V \frac{\rho_q(\vec{r}') \cdot dV'}{|\vec{r}_{\text{bound}} - \vec{r}'|}. \quad (6)$$

The integration is conducted over a region V_p where an equality $|\rho_q| \geq 0.001 \cdot |\rho_q|^{\max}$ is satisfied. Here $|\rho_q|^{\max}$ is the maximum value of the charge density within the computational domain [Bourdon *et al.*, 2007].

To calculate the photoionization source S_{ph} , the model by Luque *et al.* [2007], developed further by Bourdon *et al.* [2007], was used. In this model, the computation of the integral in the classical model by Zheleznyak *et al.* [1982] is replaced by solving three Helmholtz equations:

$$S_{ph}(\vec{r}) = \sum_{j=1}^3 S_{ph}^j(\vec{r}), \quad (7)$$

$$\Delta S_{ph}^j(\vec{r}) - (\lambda_j p_{O_2})^2 S_{ph}^j(\vec{r}) = -A_j p_{O_2}^2 I(\vec{r}),$$

where $I(\vec{r}) = \frac{p_q}{p+p_q} \zeta \frac{v_u}{v_{ion}} S_{ion}(\vec{r})$, $S_{ion}(\vec{r}) = v_{ion} n_e(\vec{r})$, $p = 1$ atm is the air pressure, p_{O_2} is the oxygen partial pressure, and p_q is the quenching pressure [Zheleznyak *et al.*, 1982]. The other symbols are defined in Bourdon *et al.* [2007].

At the boundary of the computational area, the photoionization source was calculated as follows:

$$S_{ph}^j(\vec{r}_{bound}) = A_j p_{O_2}^2 Q_{ph} \cdot \frac{\exp(-\lambda_j p_{O_2} \cdot |\vec{r}_{bound} - \vec{r}_{ph}|)}{4\pi |\vec{r}_{bound} - \vec{r}_{ph}|}, \quad (8)$$

where

$$Q_{ph} = \int_{V_{sim}} I(\vec{r}') \cdot dV' \quad \text{and} \quad \vec{r}_{ph} = \frac{\int_{V_{sim}} \vec{r}' \cdot I(\vec{r}') \cdot dV'}{Q_{ph}}.$$

The expression (8) was derived using the general solution of Helmholtz equation:

$$S_{ph}^j(\vec{r}) = \int_{V_{sim}} \frac{I(\vec{r}') A_j p_{O_2}^2 e^{-\lambda_j p_{O_2} |\vec{r} - \vec{r}'|}}{4\pi |\vec{r} - \vec{r}'|} \cdot dV'. \quad (9)$$

When deriving equation (8), we decomposed the function $\frac{e^{-\lambda_j p_{O_2} |\vec{r} - \vec{r}'|}}{|\vec{r} - \vec{r}'|}$ in equation (9) over the Taylor series in the vicinity of point \vec{r}_{ph} and retained only the zero term. This procedure is the same used in electrostatics while decomposing the electric potential over the multipoles. The integration is conducted over the entire volume of the simulation domain V_{sim} .

The number of electrons in the runaway mode $N_{re}(t)$ at the moment of time t was computed as follows:

$$N_{re}(t) = \int_0^t \int_{V_{sim}} v_{run}(E(z, r, t')) \cdot n_e(z, r, t') \cdot dV' \cdot dt', \quad (10)$$

where $v_{run}(E)$ is the rate of transition of low-energy electrons to the runaway mode. We use a dependence of the runaway rate on the field intensity calculated by Bakhov *et al.* [2000] in nitrogen of atmospheric density in the range of the field from 240 to 400 kV/cm for various magnitudes of the stochastic runaway threshold $\varepsilon_{th,run,stoch}$.

Computations were executed assuming STP conditions with the oxygen partial pressure $p_{O_2} = 0.2$ atm, the quenching pressure $p_q = 0.0395$ atm [Bourdon *et al.*, 2007], $L_0 = 4$ cm, $R_0 = 6$ mm, $E_0 = 50$ kV/cm, and $l_z = l_r = 500$ μ m. The magnitude of the initial electron density at the channel symmetry axis $n_e^{ch,a,i}$ was varied between simulations.

Initially, we need to calculate the $n_p^{ch,a,i}$ magnitude. With this goal, a preliminary problem is solved using the equation (1) without the flux terms; we let the field inside the old streamer channel be $E = 10$ kV/cm and densities at the channel symmetry axis $n_e^{ch,a}(\tau = 0) = n_p^{ch,a}(\tau = 0) = 10^{20}$ m^{-3} . The simulations are conducted until the instant of time, \tilde{t} , at which the electron density at the old streamer channel symmetry axis $n_e^{ch,a}(\tau = \tilde{t})$ achieves the given $n_e^{ch,a,i}$ magnitude. Typical values of \tilde{t} were found to be ~ 1 μ s with $n_p^{ch,a,i} = n_p^{ch,a}(\tilde{t}) \approx 5 \cdot 10^{17}$ m^{-3} . Further, while solving the full set of equation (1), we consider $\tilde{t} = 1$ μ s as the initial moment of time ($t = \tau - \tilde{t}$).

Table 1. Results of Computations

$n_e^{\text{ch,a,i}}, \text{m}^{-3}$	$t_{z_f=3 \text{ cm}}, \text{ns}$	$E_f, \text{kV/cm}$	$v_f, \text{m/s}$	$k_{\text{RE}}, 1/\text{m}$
10^{10}	3.86	205	$1.3 \cdot 10^7$	$2 \cdot 10^4$
10^{11}	3.80	267	$2 \cdot 10^7$	$5 \cdot 10^7$
10^{12}	3.66	296	$2 \cdot 10^7$	$2 \cdot 10^9$
10^{13}	3.50	286	$3 \cdot 10^7$	$9 \cdot 10^8$
10^{14}	3.31	253	$3 \cdot 10^7$	$2 \cdot 10^7$
10^{15}	3.14	204	$3 \cdot 10^7$	$3 \cdot 10^4$

For the dependencies of μ_{er} , $\mu_{p,r}$, D_{er} , v_{ionr} , β_{ep} , β_{pr} , k_{diss} , and k_{thr} on the field intensity and pressure, we follow *Bochkov et al.* [2013]. To calculate the photoionization rate, we find the parameters λ_j and A_j ($j=1-3$) in *Bourdon et al.* [2007] and the dependence of the quantity $\zeta v_u/v_{ion}$ on the field intensity in *Liu and Pasko* [2004].

The RE number $N_{re}(t)$ was computed with the stochastic runaway threshold $\varepsilon_{th,run,stoch} = 8 \text{ keV}$ using the Monte Carlo data on the runaway rate $v_{run}(E)$ available in *Bakhov et al.* [2000], which with an error, not exceeding 13%, is approximated as follows:

$$v_{run}(E) = 3.5 \cdot 10^{-24} [\text{s}^{-1}] \cdot \exp\left(- (2.166 \cdot 10^{-7} [\text{m/V}] \cdot E)^2 + 3.77 \cdot 10^{-6} [\text{m/V}] \cdot E\right). \quad (11)$$

4. Results and Discussion

The set in equation (1) was solved using the finite differences technique. To get rid of numerical diffusion while calculating the flux terms, the technique of flux-corrected transport [*Zalesak*, 1979] was used. The QUICKEST 3 [*Leonard*, 1991] and “donor cell” schemes were used, respectively, as the high-order and low-order schemes.

The time step chosen was $\Delta t = 5 \cdot 10^{-13} \text{ s}$. Adaptive mesh was accepted for the axis z : in the domain of the ionization wavefront with size of 1 cm, the spatial step was $\Delta z = 10^{-5} \text{ m}$, and in the remaining area away from the front, the step was $\Delta z = 5 \cdot 10^{-5} \text{ m}$. The domain with step $\Delta z = 10^{-5} \text{ m}$ moved consistently with the ionization wavefront propagation. Along the r axis, the mesh was uniform with constant step $\Delta r = 10^{-5} \text{ m}$. The simulations were terminated at the moment of time $t_{z_f=3 \text{ cm}}$, such that a position of the maximum of the field intensity appeared at the point with coordinate $z_f = 3 \text{ cm}$.

The results for $n_e^{\text{ch,a,i}} = 10^{10}-10^{15} \text{ m}^{-3}$ are presented in Table 1, where E_f is the maximum value of the field intensity at the ionization wavefront, v_f is the propagation velocity of the front at $t_{z_f=3 \text{ cm}}$, and k_{RE} is the number of REs produced by the ionization wave per unit length at the final section of its path from 2.9 to 3.0 cm:

$$k_{\text{RE}} = \frac{N_{\text{RE}}(t_{z_f=3 \text{ cm}}) - N_{\text{RE}}(t_{z_f=2.9 \text{ cm}})}{0.1 \text{ cm}}. \quad (12)$$

The field intensity and electron density on the symmetry axis at various moments of time are shown in Figure 3 for $n_e^{\text{ch,a,i}} = 10^{12} \text{ m}^{-3}$. Two-dimensional distributions at $t_{z_f=3 \text{ cm}} = 3.6 \text{ ns}$ are illustrated in Figure 4. It is seen that, although the primary channel is significantly expended as a result of the ionization wave development, the transverse size of the front domain with the field intensity close to the runaway threshold $\sim 240 \text{ kV/cm}$ remains almost the same as the characteristic size of the primary channel $l_r = 500 \mu\text{m}$ (cf., Figure 2).

It is seen from the data in Table 1 that with increasing preionization level, given by $n_e^{\text{ch,a,i}}$, the maximum value of the field intensity E_f at the ionization wavefront increases as we expected. However, when $n_e^{\text{ch,a,i}}$ gets too high, the initial electron conductivity tends to reduce the accumulated space charge density at the wavefront; as a result, E_f decreases with $n_e^{\text{ch,a,i}}$ increase as seen for $n_e^{\text{ch,a,i}} > 10^{13} \text{ m}^{-3}$. This decrease has been observed in other works that look at the effects of the increase of the photoionization level with altitude [*Liu and Pasko*, 2004; *Luque et al.*, 2007; *Chanrion and Neubert*, 2008] or at the effect of the ionization from high-energy electrons ahead of the streamer [*Chanrion et al.*, 2014]. We also point out that the photoionization in air at ground pressure produces electron density of 10^{13} m^{-3} at the vicinity of the wavefront [*Bazelyan and Raizer*, 1998, 1997, page 92] which is within the range of the used magnitudes of the preionization level, $n_e^{\text{ch,a,i}}$. However, the ionization by electron impacts in the front dominates because we analyze the proforce ionization wave, i.e., propagating along $-e\vec{E}$.

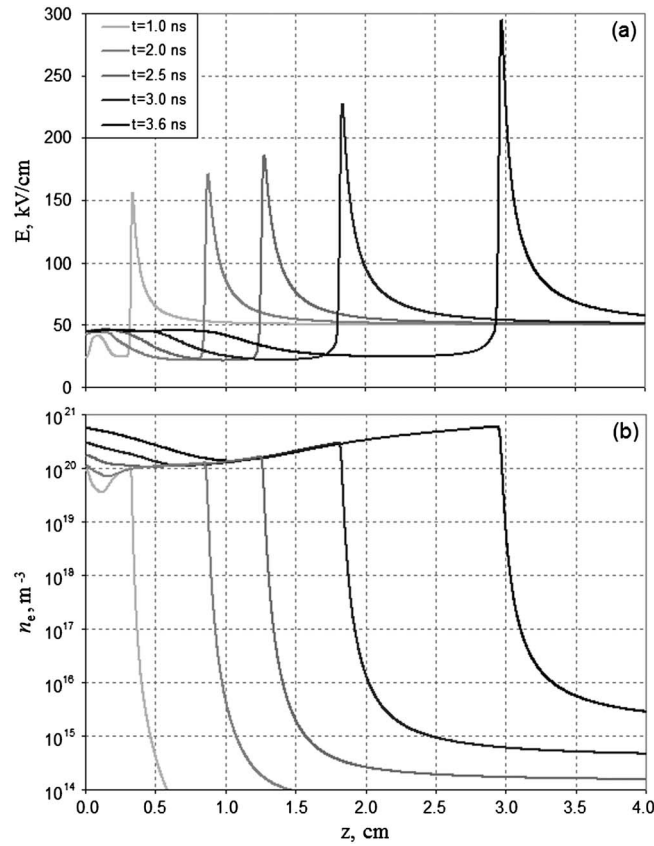


Figure 3. (a) The field intensity and (b) the electron density along the channel symmetry axis for the initial electron concentration $n_e^{ch,a,i} = 10^{12} m^{-3}$ at various moments of time.

about $N_{str} \approx 1.2 \cdot 10^5$ streamers develop in a streamer zone within the radius of $R_s \approx 1.5$ m of a leader head at a potential $U_L = 1.5$ MV. The lifetime t_{life} of one streamer propagating with a minimum velocity $v_{s,min} \sim 10^5$ m/s is of $t_{life} \sim R_s / v_{s,min} \sim 10 \mu s$. Only in channels of relatively young streamers, developing during time \tilde{t} in the range $\Delta \tilde{t} = 1.4\text{--}2.3 \mu s$ (corresponding to $n_e^{ch,a,i} = 10^{14}\text{--}10^{11} m^{-3}$ at which $E_f > 240$ kV/cm) up to a length $l_s = \tilde{t} \cdot v_{s,min} \approx 10\text{--}20$ cm, the electron density is sufficient to start new ionization wave-generating REs. Note that we let streamer radius changes weakly relative to the initial radius $l_r = 500 \mu m$. If the streamer becomes much wider, we can assume that the streamer branches. The radii of the branches are less than that of the parent streamer; therefore, the processes of field enhancement and electron acceleration continue at the branch heads.

With the above considerations, we estimate the number of REs generated in a leader step $N_{RE} \approx l_s \cdot k_{RE} \cdot (\Delta \tilde{t} / t_{life}) N_{str} \sim 10^{12}$, where we have assumed that the ionization waves propagate about 10% of the streamer length, $(\Delta \tilde{t} / t_{life}) \approx 0.1$. The leader potential is probably considerably higher than the 1.5 MV used by *Bazelyan and Raizer* [2000, 2001, page 76]; therefore, the number of REs generated by lightning discharges is likely larger. Note that the above estimation, $N_{RE} \approx 10^{12}$, is rather close to estimated by *Babich et al.* [2013] numbers $10^{10} - 4 \cdot 10^{11}$ of high-energy REs generated by one leader step, which are required for reproducing the X-ray energy of $\sim 1\text{--}2$ MeV measured by *Dwyer et al.* [2005].

We only simulated a single streamer, with ambient empty space around it. In reality, the corona consists of multiple streamers developing simultaneously. There is a chance that they affect each other and modify the electric field. Ignoring this fact is a shortcoming inherent for the available models [*Moss et al.*, 2006; *Celestin and Pasko*, 2011; *Bazelyan and Raizer*, 2000, 2001, chap. 2], considering a development of a single streamer in the corona. The single-streamer approximation is substantiated

It is seen from Table 1 that with $n_e^{ch,a,i} = 10^{11}\text{--}10^{14} m^{-3}$, the field intensity is $\sim 250\text{--}300$ kV/cm and within the range required for efficient RE generation; on the order of $\sim 10^7\text{--}10^9$ electrons/m are estimated with energies above the stochastic runaway threshold $\epsilon_{th,run,stoch} = 8$ keV [*Bakhov et al.*, 2000]. From these values, it is possible to estimate a number of REs generated by one leader step. Note, however, that two uncertainties are inevitable, for such estimation. First, the number of streamers with front field sufficiently strong for the RE generation a priori is not known—only rather uncertain estimates are possible. Second, there is an uncertainty connected with the extremely strong dependence of the number of REs on the field intensity, which, obviously, at each instant of time, strongly varies in different streamers constituting the corona. In fact, the runaway probability varies 7 orders of magnitude for E/E_k increasing from 6 to 9 [*Chanrion and Neubert*, 2010].

Proceeding, with these cautions in mind, to estimate the number of REs expected from a lightning leader step, we note that according to *Bazelyan and Raizer* [2000, 2001, page 77],

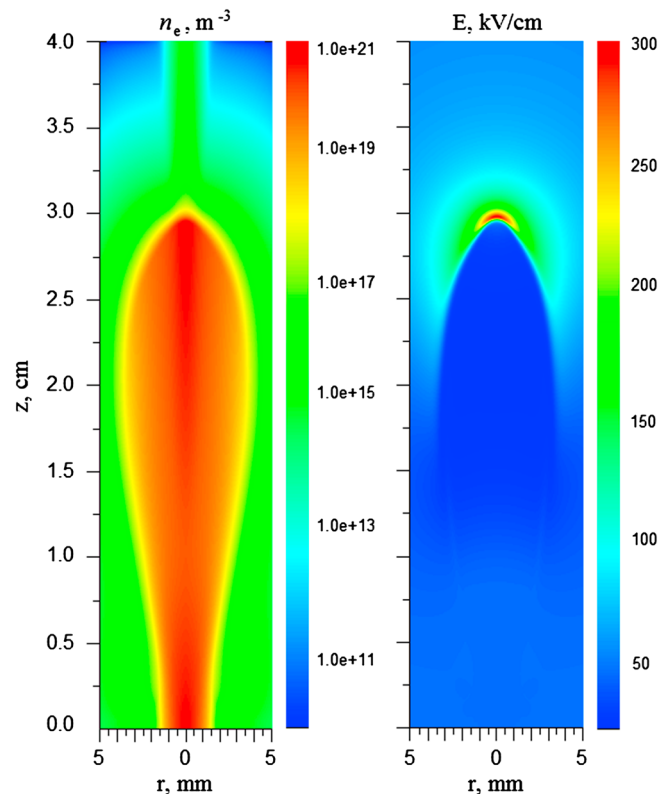


Figure 4. The spatial distribution of (left) the electron density and (right) the field intensity at $t = 3.6$ ns for $n_e^{\text{ch,a,l}} = 10^{12} \text{ m}^{-3}$.

the ionization wave to the channel, thereby enhancing the peak field in the ionization wave. The inhomogeneity is important for transverse scales of the order of the radius of a streamer head dimension.

Numerical simulations were executed in a self-consistent electric field allowing for the drift motion of electrons and positive and negative ions, and for electron diffusion, impact ionization of air molecules by low-energy electrons, recombination, attachment of low-energy electrons to the oxygen molecules, and photoionization of the air. We demonstrated that with characteristic size $500 \mu\text{m}$ of the initial spatial distribution of the electron density with maximum magnitudes in the range from 10^{11} to 10^{14} m^{-3} , an electric field with intensity $250\text{--}300 \text{ kV/cm}$, corresponding to $E/E_k \sim 8\text{--}10$, is produced in an ionization wave launched by an impulsive increase in the electric potential. The enhancement is sufficient for electrons to reach the runaway mode and, consequently, for producing the X-ray and γ ray pulses observed in correlation with the lightning leader steps [Dwyer *et al.*, 2005]. The estimated number of runaway electrons is consistent with the numbers required [Babich *et al.*, 2013] for reproducing the X-ray energy generated by stepped leader [Dwyer *et al.*, 2005]. We predict that the RE numbers generated by lightning exceed 10^{12} by a large factor.

References

- Babaeva, N. Y., and G. V. Naidis (1996), Two-dimensional modeling of positive streamer dynamics in nonuniform electric fields in air, *J. Phys. D Appl. Phys.*, *29*, 2423.
- Babich, L. P. (1995), Bistability of electron ensemble interacting with dense gas of neutral particles in electric field: Application to thunderclouds fields, *High Temp.*, *33*(5), 653–656, Original Russian text published in *Teplofizika Vysokih Temperatur* *33*, 659.
- Babich, L. P. (2003), *High Energy Phenomena in Electric Discharges in Dense Gases: Theory, Experiment and Natural Phenomena*, Futurepast Inc., Arlington, Va.
- Babich, L. P. (2005), Analysis of a new electron-runaway mechanism and record-high runaway-electron currents achieved in dense-gas discharges, *Phys.-Usp.*, *48*, 1015–1037, doi:10.1070/PU2005v048n10ABEH002805.
- Babich, L. P., and E. I. Bochkov (2011), Deterministic methods for numerical simulation of high-energy runaway electron avalanches, *J. Exp. Theor. Phys.*, *112*, 494–503, doi:10.1134/S1063776111020014, Original Russian text published in *ZhETF* *139*, 568–578.
- Babich, L. P., and T. V. Loiko (2009), Subnanosecond pulses of runaway electrons generated in atmosphere by high-voltage pulses of microsecond duration, *Dokl. Phys.*, *54*, 479–482, doi:10.1134/S1028335809110019.

by Bazelyan and Raizer [2000, 2001, page 78], who estimated that $N_{\text{str}} \approx 1.2 \cdot 10^5$ streamers developing in a streamer zone with size $R \approx 1.5$ m are sufficiently distant from each other and can be considered as lonely, developing in the self-consistent electric field combining the front leader field and the field of the considered streamer. Nevertheless, accurate analyses are required of multistreamer problem.

5. Conclusion

We have shown that the inhomogeneous environment of a negative lightning leader may lead to impulsive electric field enhancement to magnitudes allowing acceleration of low-energy electrons to runaway energies. The high fields are created because the ionization wave speed depends not only on the ionization rate $v_{\text{ion}}(E)$ but also on the ionization degree of the ambient plasma, being generally lower at lower plasma densities. If preionized streamer channels are present in front of the leader, this effect tends to focus

Acknowledgments

The VNIIEF coauthors express the deepest gratitude to C. Haldoupis who, in cooperation with T. Neubert, has been an international collaborator in the completed ISTC project 3993–2010, within the framework of which this work was being carried out, to N. Crosby, S. Cummer, A. van Deursen, J.R. Dwyer, R. Roussel-Dupré, D. Smith, T. Torii, and E. Williams for their support of the project proposal. They thank R.A. Roussel-Dupré and E.M.D. Symbalisty for the long-term collaboration, the continuation of which is this paper. The authors would like to thank the reviewers whose invaluable comments have allowed significant improvement of this paper. Readers can access the data from the paper via authors by emails: babich@elph.vniief.ru and Neubert@space.dtu.dk. The work has benefitted from collaborations within the European Science Foundation (ESF) Research Networking Project “Thunderstorm Effects on the Atmosphere-Ionosphere System” (TEA-IS).

Alan Rodger thanks Nikolai G. Lehtinen and another reviewer for their assistance in evaluating this paper.

- Babich, L. P., and Y. L. Stankevich (1972), Transition from streamers to continuous electron acceleration, *Sov. Phys. Tech. Phys.*, *17*, 1333–1336.
- Babich, L. P., T. V. Loiko, and V. A. Tsukerman (1990), High-voltage nanosecond discharges in a dense gas at a high overvoltage with runaway electrons, *Sov. Phys. Usp.*, *33*, 521–540.
- Babich, L. P., E. N. Donskoy, R. I. Il'kaev, I. M. Kutsyk, and R. A. Roussel-Dupré (2004), Fundamental parameters of a relativistic runaway electron avalanche in air, *Plasma Phys. Rep.*, *30*, 616–624, Original Russian text published in *Fizika Plazmy* *30*, 666–674.
- Babich, L. P., E. N. Donskoi, and I. M. Kutsyk (2008), Analysis of atmospheric gamma-ray flashes detected in near space with allowance for the transport of photons in the atmosphere, *J. Exp. Theor. Phys.*, *107*, 49–60.
- Babich, L. P., E. I. Bochkov, E. N. Donskoi, and I. M. Kutsyk (2010), Source of prolonged bursts of high-energy gamma-rays detected in thunderstorm atmosphere in Japan at the coastal area of the Sea of Japan and on high mountain top, *J. Geophys. Res.*, *115*, A09317, doi:10.1029/2009JA015017.
- Babich, L. P., I. M. Kutsyk, E. N. Donskoi, and J. R. Dwyer (2013), Analysis of the experiment on registration of X-rays from the stepped leader of a cloud-to-ground lightning discharge, *J. Geophys. Res. Space Physics*, *118*, 2573–2582, doi:10.1002/jgra.50236.
- Babich, L. P., T. V. Loiko, and A. V. Rodigin (2014a), Calibration of detectors of ionizing emissions by means of subnanosecond runaway electron beam generated by discharge in open atmosphere at high overvoltages, *Instrum. Exp. Tech.*, *57*(3), 248–254, Original Russian text published in *Pribory i Tekhnika Eksperimenta*, 2014, no. 3, 21–27.
- Babich, L. P., T. V. Loiko, and A. V. Rodigin (2014b), The first observations of Cherenkov's radiation of runaway electrons produced by discharge in dense gas, *IEEE Trans. Plasma Sci.*, *42*(4), 948–952, doi:10.1109/TPS.2014.2308529.
- Bakhov, I. K., L. P. Babich, and I. M. Kutsyk (2000), Temporal characteristics of runaway electrons in electron-neutral collision dominated plasma of dense gases. Monte Carlo calculations, *IEEE Trans. Plasma Sci.*, *28*, 1254–1262.
- Bazelyan, E. M., and Y. P. Raizer (1997), *Iskrovoi razryad*, MPhTI, Moscow [in Russian]; (1998), *Spark discharge*, NY: Chemical Rubber Company Press.
- Bazelyan, E. M., and Y. P. Raizer (1998), *Spark Discharge*, CRC Press, Boca Raton, Fla.
- Bazelyan, E. M., and Y. P. Raizer (2000), *Lightning Physics and Lightning Protection*, IOP Publishing, Bristol, England.
- Bazelyan, E. M., and Y. P. Raizer (2001), *Fizika molnii i molniezaschita*, Fizmatlit, Moscow [in Russian]; (2000), *Lightning Physics and Lightning Protection*, IOP Publishing, Bristol.
- Biagi, C. J., M. A. Uman, J. D. Hill, D. M. Jordan, V. A. Rakov, and J. Dwyer (2010), Observations of stepping mechanisms in a rocket-and-wire triggered lightning flash, *J. Geophys. Res.*, *115*, D23215, doi:10.1029/2010JD014616.
- Bochkov, E. I., L. P. Babich, and I. M. Kutsyk (2013), Numerical simulation of narrow bipolar electromagnetic pulses generated by thunderstorm discharges, *J. Exp. Theor. Phys.*, *117*, 177–184, doi:10.1134/S106377611308013X, Original Russian text published in *ZhETF* *144*, 205–214.
- Bourdon, A., V. P. Pasko, N. Y. Liu, S. Celestin, P. Segur, and E. Marode (2007), Efficient models for photoionization produced by non-thermal gas discharges in air based on radiative transfer and the Helmholtz equations, *Plasma Sources Sci. Technol.*, *16*, 656–678.
- Briggs, M. S., et al. (2010), First results on terrestrial gamma ray flashes from the Fermi Gamma-ray Burst Monitor, *J. Geophys. Res.*, *115*, A07323, doi:10.1029/2009JA015242.
- Briggs, M. S., et al. (2011), Electron-positron beams from terrestrial lightning observed with Fermi-GBM, *Geophys. Res. Lett.*, *38*, L02808, doi:10.1029/2010GL046259.
- Brunetti, M., S. Cecchini, M. Galli, G. Giovannini, and A. Pagliarini (2000), Gamma-ray bursts of atmospheric origin in the MeV energy range, *Geophys. Res. Lett.*, *27*, 1599–1602, doi:10.1029/2000GL003750.
- Celestin, S., and V. P. Pasko (2011), Energy and fluxes of thermal runaway electrons produced by exponential growth of streamers during the stepping of lightning leaders and in transient luminous events, *J. Geophys. Res.*, *116*, A03315, doi:10.1029/2010JA01626.
- Chanrion, O., and T. Neubert (2008), A PIC-MCC code for simulation of streamer propagation in air, *J. Comput. Phys.*, *227*(15), 7222–7245, doi:10.1016/j.jcp.2008.04.016.
- Chanrion, O., and T. Neubert (2010), Production of runaway electrons by negative streamer discharges, *J. Geophys. Res.*, *115*, A00E32, doi:10.1029/2009JA014774.
- Chanrion, O., Z. Bonaventura, D. Çinar, A. Bourdon, and T. Neubert (2014), Runaway electrons from a 'beam-bulk' model of streamer: Application to TGFs, *Environ. Res. Lett.*, *9*, 055003, doi:10.1088/1748-9326/9/5/055003.
- Chilingarian, A., A. Daryan, K. Arakelyan, A. Hovhannisyanyan, B. Mailyan, L. Melkumyan, G. Hovsepian, S. Chilingaryan, N. Bostanjyan, and A. Reymers (2009), Discovery of the thunderstorm correlated fluxes of electrons, gammas and neutrons observed at mountain altitudes, *Proc. 31-th International Cosmic Ray Conf.*, Lodz, Poland.
- Chilingarian, A., G. Hovsepian, and A. Hovhannisyanyan (2011), Particle bursts from thunderclouds: Natural particle accelerators above our heads, *Phys. Rev. D*, *83*(6, 062001), doi:10.1103/PhysRevD.83.062001.
- Chilingaryan, A., A. Daryan, K. Arakelyan, A. Hovhannisyanyan, B. Mailyan, L. Melkumyan, G. Hovsepian, S. Chilingaryan, A. Reymers, and L. Vanyan (2010), Ground-based observations of thunderstorm-correlated fluxes of high-energy electrons, gamma rays, and neutrons, *Phys. Rev. D*, *82*, 043009.
- Cohen, M. B., U. S. Inan, and G. Fishman (2006), Terrestrial gamma ray flashes observed aboard the Compton Gamma Ray Observatory/Burst and Transient Source Experiment and ELF/VLF radio atmospheric, *J. Geophys. Res.*, *111*, D24109, doi:10.1029/2005JD006987.
- Cummer, S. A., Y. Zhai, W. Hu, D. M. Smith, L. I. Lopez, and M. A. Stanley (2005), Measurements and implications of the relationship between lightning and terrestrial gamma ray flashes, *Geophys. Res. Lett.*, *32*, L08811, doi:10.1029/2005GL022778.
- Dwyer, J. R. (2003a), Energetic radiation produced during rocket-triggered lightning, *Science*, *299*, 694–697.
- Dwyer, J. R. (2003b), A fundamental limit on electric fields in air, *Geophys. Res. Lett.*, *30*(20), 2055, doi:10.1029/2003GL017781.
- Dwyer, J. R. (2004), Implications of X-ray emission from lightning, *Geophys. Res. Lett.*, *31*, L12102, doi:10.1029/2004GL019795.
- Dwyer, J. R. (2007), Relativistic breakdown in planetary atmospheres, *Phys. Plasmas*, *14*(4), 042901, doi:10.1063/1.2709652.
- Dwyer, J. R. (2008), The source mechanisms of terrestrial gamma-ray flashes, *J. Geophys. Res.*, *113*, D10103, doi:10.1029/2007JD009248.
- Dwyer, J. R. (2012), The relativistic feedback discharge model of terrestrial gamma ray flashes, *J. Geophys. Res.*, *117*, A02308, doi:10.1029/2011JA017160.
- Dwyer, J. R., and D. M. Smith (2005), A comparison between Monte Carlo simulations of runaway breakdown and terrestrial gamma-ray flash observations, *Geophys. Res. Lett.*, *32*, L22804, doi:10.1029/2005GL023848.
- Dwyer, J. R., et al. (2004), A ground level gamma-ray burst observed in association with rocket-triggered lightning, *Geophys. Res. Lett.*, *31*, L05119, doi:10.1029/2003GL018771.
- Dwyer, J. R., et al. (2005), X-ray bursts associated with leader steps in cloud-to-ground lightning, *Geophys. Res. Lett.*, *32*, L01803, doi:10.1029/2004GL021782.
- Dwyer, J. R., M. Schaal, H. K. Rassoul, M. A. Uman, D. M. Jordan, D. Hill, and H. K. Rassoul (2011), High-speed X-ray images of triggered lightning dart leaders, *J. Geophys. Res.*, *116*, D20208, doi:10.1029/2011JD015973.

- D'yakov, M. I., and I. Y. Kocharovskiy (1988), Stationary streamer propagation in electronegative gas [in Russian], *ZhETP*, *94*, 32.
- D'yakov, M. I., and I. Y. Kocharovskiy (1989), On the streamer discharge in homogeneous field [in Russian], *ZhETP*, *95*, 1850.
- Eack, K. B., W. H. Beasley, W. D. Rust, T. C. Marshall, and M. Stolzenburg (1996a), Initial results from simultaneous observation of X-rays and electric fields in a thunderstorm, *J. Geophys. Res.*, *101*, 29,637–29,640, doi:10.1029/96JD01705.
- Eack, K. B., W. H. Beasley, W. D. Rust, T. C. Marshall, and M. Stolzenburg (1996b), X-ray pulses observed above a mesoscale convective system, *Geophys. Res. Lett.*, *23*, 2915–2918, doi:10.1029/96GL02570.
- Eack, K. B., D. M. Suszcynsky, W. B. Beasley, R. A. Roussel-Dupre, and E. M. Symbalysty (2000), Gamma-ray emissions in a thunderstorm anvil, *Geophys. Res. Lett.*, *27*, 185–188, doi:10.1029/1999GL010849.
- Fishman, G. J., et al. (1994), Discovery of intense gamma-ray flashes of atmospheric origin, *Science*, *264*, 1313–1316.
- Gorin, B. N., V. I. Levitov, and A. V. Shkilev (1976), Some principles of leader discharge of air gaps with a strong non-uniform field, *IEEE Conf. Publ.*, *143*, 274–278.
- Gurevich, A. V. (1961), To the theory of the effect of the runaway electrons, *Sov. Phys. JETP*, *12*, 904, Original Russian text published in *ZhETP* *39*, 1296–1301.
- Gurevich, A. V., G. M. Milikh, and R. A. Roussel-Dupre (1992), Runaway electron mechanism of air breakdown and preconditioning during a thunderstorm, *Phys. Lett. A*, *165*, 463–468.
- Gurevich, A. V., K. P. Zybin, and Y. V. Medvedev (2007), Runaway breakdown in strong electric field as a source of terrestrial gamma flashes and gamma bursts in lightning leader steps, *Phys. Lett. A*, *361*, 119–125.
- Howard, J., M. A. Uman, J. R. Dwyer, D. Hill, C. Biagi, Z. Saleh, J. Jerauld, and H. K. Rassoul (2008), Co-location of lightning leader X-ray and electric field change sources, *Geophys. Res. Lett.*, *35*, L13817, doi:10.1029/2008GL034134.
- Khaerdinov, N. S., A. S. Lidvansky, and V. B. Petkov (2005), Cosmic rays and the electric field of thunderclouds: Evidence for acceleration of particles (runaway electrons), *Atmos. Res.*, *76*, 246–354.
- Kochkin, P. O., C. V. Nguyen, A. P. J. van Deursen, and U. Ebert (2012), Experimental study of hard X-rays emitted from meter-scale positive discharges in air, *J. Phys. D Appl. Phys.*, *45*, 425202, doi:10.1088/0022-3727/45/42/425202.
- Kulikovskiy, A. A. (1997), Two-dimensional simulation of the positive streamer in N₂ between parallel-plate electrodes, *Phys. D: Appl. Phys.*, *30*, 441.
- Kulikovskiy, A. A. (1998), Three-dimensional simulation of a positive streamer in air near curved anode, *Phys. Lett. A*, *245*, 445.
- Kutsyk, I. M., L. P. Babich, E. N. Donskoi, and E. I. Bochkov (2012a), Numerical analysis of the concept of a laboratory experiment on the demonstration of runaway electron breakdown under normal conditions at high overvoltages, *JETP Lett.*, *95*, 631–636, doi:10.1134/S0021364012120090, Original Russian text published in *ZhETF Lett.* *2012*, *95*, 712–717.
- Kutsyk, I. M., L. P. Babich, E. N. Donskoi, and E. I. Bochkov (2012b), Analyses of a laboratory experiment on the observation of runaway electron avalanche in air at high overvoltages, *Plasma Phys. Rep.*, *38*, 891–898, doi:10.1134/S1063780X12110050, Original Russian text published in *Fizika Plazmy* *38*, 969–976.
- Lehtinen, N. G., T. F. Bell, and U. S. Inan (1999), Monte Carlo simulation of runaway MeV electron breakdown with application to red sprites and terrestrial gamma ray flashes, *J. Geophys. Res.*, *104*, 24,699–24,712, doi:10.1029/1999JA900335.
- Leonard, B. P. (1991), The ULTIMATE conservative difference scheme applied to unsteady one-dimensional advection, *Comp. Math. In: Applied Mech. and Eng.*, *88*, 17–74.
- Liu, N., and V. P. Pasko (2004), Effects of photoionization on propagation and branching of positive and negative streamers in sprites, *J. Geophys. Res.*, *109*, A04301, doi:10.1029/2003JA010064.
- Luque, A., U. Ebert, C. Montijn, and W. Hundsdorfer (2007), Photoionization in negative streamers: Fast computations and two propagation modes, *Appl. Phys. Lett.*, *90*, 081501, doi:10.1063/1.2435934.
- Mallios, S. A., S. Celestin, and V. P. Pasko (2013), Production of very high potential differences by intracloud lightning discharges in connection with terrestrial gamma ray flashes, *J. Geophys. Res. Space Physics*, *118*, 912–918, doi:10.1002/jgra.50109.
- McCarthy, M., and G. K. Parks (1985), Further observations of X-rays inside thunderstorms, *Geophys. Res. Lett.*, *12*, 393–396, doi:10.1029/GL012i006p00393.
- Moore, C. B., K. B. Eack, G. D. Aulich, and W. Rison (2001), Energetic radiation associated with lightning stepped-leaders, *Geophys. Res. Lett.*, *28*, 2141–2144, doi:10.1029/2001GL013140.
- Moss, G. D., V. P. Pasko, N. Liu, and G. Veronis (2006), Monte Carlo model for analysis of thermal runaway electrons in streamer tips in transient luminous events and streamer zones of lightning leaders, *J. Geophys. Res.*, *111*, A02307, doi:10.1029/2005JA011350.
- Neubert, T., and O. Chanrion (2013), On the electric breakdown field of the mesosphere and the influence of electron detachment, *Geophys. Res. Lett.*, *40*, 2373–2377, doi:10.1002/grl.50433.
- Noggle, R. C., E. P. Krider, and J. R. Wayland (1968), A search for X-rays from helium and air discharges at atmospheric pressure, *J. Appl. Phys.*, *39*, 4746–4748.
- Peterson, L. R., and A. E. S. Green (1968), The relation between ionization yields, cross sections and loss functions, *J. Phys. B: At. Mol. Phys.*, *1*, 1131–1140.
- Raizer, Y. P., and A. N. Simakov (1998), What determines the radius and maximum field at the leader head of long streamers? [in Russian], *Fizika Plazmy (Plasma Physics Reports)*, *24*, 754.
- Reess, T., P. Ortega, A. Gibert, P. Domens, and P. Pignolet (1995), An experimental study of negative discharge in a 1.3 m point-plane air gap: The function of the space stem in the propagation mechanisms, *J. Phys. D Appl. Phys.*, *28*, 2306–2313, doi:10.1088/0022-3727/28/11/011.
- Roussel-Dupre, R. A., A. V. Gurevich, T. Tunnell, and G. M. Milikh (1994), Kinetic theory of runaway air breakdown, *Phys. Rev. E*, *49*(3), 2257–2271.
- Shaw, G. E. (1967), Background cosmic count increases associated with thunderstorms, *J. Geophys. Res.*, *72*, 4623–4626, doi:10.1029/JZ072i018p04623.
- Smith, D. M., L. I. Lopez, R. P. Lin, and C. P. Barrington-Leigh (2005), Terrestrial gamma-ray flashes observed up to 20 MeV, *Science*, *307*, 1085–1088.
- Stankevich, Y. L., and V. G. Kalinin (1967), Fast electrons and X-rays in the initial stage of pulsed spark discharge, *Sov. Phys. Dokl.*, *12*, 1042, Original Russian text published in *Doklady Akademii Nauk SSSR* *117*, 72–73, 1967.
- Suszcynsky, D. M., R. Roussel-Dupre, and G. Shaw (1996), Ground-based search for X-rays generated by thunderstorms and lightning, *J. Geophys. Res.*, *101*, 23,505–23,516, doi:10.1029/96JD02134.
- Tarasova, L. V., and L. N. Khudyakova (1969), X-rays of pulsed discharges in air, *Sov. Tech. Phys.*, *14*, 1148–1151, Original Russian text published in *Zh. Techn. Fiz.* *39*, 1530–1533, 1969.
- Tarasova, L. V., L. N. Khudyakova, T. V. Loiko, and V. A. Tsukerman (1975), Fast electrons and X-rays from nanosecond pulsed discharges at pressures 0.1–760 torr, *Sov. Phys. Tech. Phys.*, *19*, 351, Original Russian text published in *Zh. Techn. Fiz.* *44*, 564–568, 1974.
- Tavani, M., et al. (2011), Terrestrial gamma-ray flashes as powerful particle accelerators, *Phys. Rev. Lett.*, *106*, 018501, doi:10.1103/PhysRevLett.106.01851.

- Torii, T., T. Sugita, S. Tanabe, Y. Kimura, M. Kamogawa, K. Yajima, and H. Yasuda (2009), Gradual increase of energetic radiation associated with thunderstorm activity at the top of Mt. Fuji, *Geophys. Res. Lett.*, *36*, L13804, doi:10.1029/2008GL037105.
- Torii, T., T. Sugita, M. Kamogawa, Y. Watanabe, and K. Kusunoki (2011), Migrating source of energetic radiation generated by thunderstorm activity, *Geophys. Res. Lett.*, *38*, L24801, doi:10.1029/2011GL049731.
- Tsuchiya, H., et al. (2007), Detection of high-energy gamma rays from winter thunderclouds, *Phys. Rev. Lett.*, *99*, 165002, week ending 19 October 2007.
- Tsuchiya, H., et al. (2009), Observation of an energetic radiation burst from mountain-top thunderclouds, *Phys. Rev. Lett.*, *102*, 255003, week ending 26 June 2009.
- Tsuchiya, H., et al. (2011), Long-duration γ ray emissions from 2007 and 2008 winter thunderstorms, *J. Geophys. Res.*, *116*, D09113, doi:10.1029/2010JD015161.
- Tsuchiya, H., et al. (2012), Observation of thundercloud-related gamma rays and neutrons in Tibet, *Phys. Rev. D*, *85*, 092006, ArXiv:12042578.v.1 [physics.geo.ph] 11 Apr 2012.
- Vitello, P. A., B. M. Penetrante, and J. N. Bardsley (1994), Simulation of negative streamer dynamics in nitrogen, *Phys. Rev. E*, *49*, 5574.
- Wilson, C. T. R. (1924), The acceleration of β -particles in strong electric fields such as those of thunderclouds, *Proc. Cambridge Phil. Soc.*, *22*, 534–538.
- Zalesak, S. T. (1979), Fully multidimensional flux-corrected transport algorithms for fluids, *J. Comput. Phys.*, *31*, 335–365.
- Zheleznyak, M. V., A. K. Mnatsakanyan, and S. V. Sizykh (1982), Photoionization of the nitrogen and oxygen mixtures by the gas-discharge radiation [in Russian], *Teplofizika Vysokih Temp. (High Temperature)*, *20*, 423–428.